Synthesis, characterization, antimicrobial and cytotoxic activity of novel half-sandwich Ru(II) arene complexes with benzoylthiourea derivatives

Dragiša Obradović[a], Stefan Nikolić[b], Ivana Milenković[c], Marina Milenković[c], Predrag Jovanović[d], Vladimir Savić[d], Alexander Roller[e] Marija Đorđić Crnogorac[f], Tatjana Stanojković[f], Sanja Grgurić-Šipka[a*]

[a] Faculty of Chemistry, University of Belgrade, Studentski trg 12-16, Serbia

[b] Innovative Centre Faculty of Chemistry Belgrade, University of Belgrade, Studentski trg 12-16, Serbia

[c] Department of Microbiology and Immunology, Faculty of Pharmacy, University of Belgrade, Vojvode Stepe 450, Serbia

[d] Department of Organic Chemistry, Faculty of Pharmacy, University of Belgrade, Vojvode Stepe 450, Serbia

[e] Institute of Inorganic Chemistry, Faculty of Chemistry, University of Vienna, Währinger Straße 42, Austria

[f] Institute of Oncology and Radiology of Serbia, Pasterova 14 Belgrade, Serbia

[*]Corresponding author: Sanja Grgurić-Šipka, e-mail: sanjag@chem.bg.ac.rs

Abstract

Three new ruthenium(II)-arene complexes, [Ru(η^6-p-cymene)(L^1)Cl_2] **(C1)** where L^1 is N-((4 methoxyphenyl)carbamothioyl)benzamide; [Ru(η^6-p-cymene)(L^2)Cl_2] **(C2)** where L^2 is 4-(3-benzoylthioureido)benzoic acid and [Ru(η^6-p-cymene)(L^3)Cl_2] **(C3)** where L^3 is methyl 4-(3-benzoylthioureido)benzoate have been synthetized, characterized and evaluated for their antimicrobial and anticancer activity. Characterization was performed using ^{1}H and ^{13}C NMR, IR spectroscopy, mass spectrometry, electrical conductivity measurements and X-Ray diffraction analysis. X-Ray diffraction analysis of **C1** showed typical expected "piano-stool" geometry with ruthenium coordinated to ligand via nitrogen and sulfur atoms of benzoylthiourea derivatives. Interesting, in herein described complex, upon coordination the four-membered ring was formed, instead of six-membered chelate common for this type of ligands. Cytotoxic activity was determined in human cervix adenocarcinoma (HeLa) cell line and IC_{50} values ranged from 29.68 to 52.36 μM and the complexes were more active than related ligands (except in case of C2 where it is found that IC_{50} value is close to IC_{50} value of related ligand). Complex [Ru(η^6-p-cymene)(L^1)Cl_2] **(C1)** expressed the highest cytotoxic activity with IC_{50} value of 29.7 μM. Complexes and ligands were tested against nine gram-positive and gram-negative bacteria and one yeast- *Candida albicans*. Clinical Candida spp. strains from biochemical laboratories were included in testing processes as well. Minimum inhibitory concentrations values ranged from 62.5 μg/ml for complexes against *Candida albicans* to over 1000 μg/ml for several bacteria samples.

Keywords: Antimicrobial activity, Benzylthiourea derivatives, Cytotoxic activity, Ruthenium(II) complexes

1. Introduction

Cancer caused about 9 million deaths worldwide in 2018 and it is estimated that by 2030 cancer mortality rate worldwide will rise up to 12 million annually. Official World Cancer Day, the February 4th was declared with the aim to rise up awareness of cancer and to encourage its prevention, detection and treatment. Growing problem in this area of medicine initiated intensive research with goal to discover novel anticancer drugs including metal-based ones. The most important metal-based anticancer drug is *cisplatin*, discovered in 1965 [1]. Since then, enourmous efforts of chemists have been put into metal complexes, but, unfortunately, only two more compounds are used in clinics worldwide: the platinum complex of the second generation - *carboplatin* and the third generation - *oxaliplatin* (Figure 1). They were approved in 1993 and 2002 respectively [2, 3]

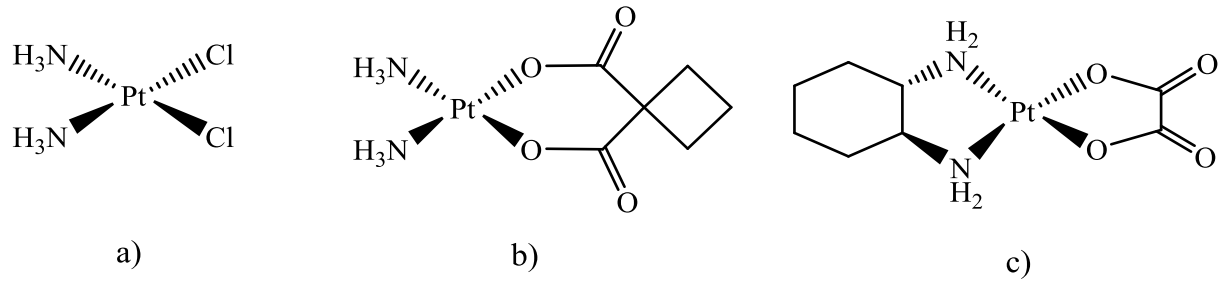

Figure 1: a) Cisplatin b) Carboplatin c) Oxaliplatin

However, application of these compounds is limited due to acquired drug resistance and toxicity to non-tumorigenic-cells causing undesirable side effects such as allergic reactions, nephrotoxicity, neurotoxicity, hepatotoxicity, hemolytic anemia, hair loss, disorder of electrolyte concentrations, nausea, decrease immunity to infections, gastrointestinal disorders, hemorrhage, hearing loss and other side effects [1].

The search for more efficient and less toxic anticancer drug has included many other metal based compounds. Among them, the ruthenium-based anticancer agents showed the greatest potential [4]. Two ruthenium compounds, NAMI-A (imidazolium trans-[tetrachlorido(1H-imidazole)(S-dimethyl sulfoxide)ruthenate(III)]) and KP1019 (indazolium trans-[tetrachloridobis(1H-indazole)ruthenate(III)]) (also studied as its more water soluble sodium salt NKP1339) (Figure 2), have been evaluated in clinical trials [5, 6]. The combinatory therapy using NAMI-A and gemcitabine is in phase II of clinical trial for the treatment of non-small cell lung carcinoma [7]. KP1019 is effective against primary cancers [8] and is another Ru-based anticancer compound entered clinical trials and the results of the early clinical development demonstrated that five out of six evaluated patients experienced disease stabilization with no severe side effects [9]. Since the mechanism of action of those drug candidates included the reduction of metal to Ru(II) form [10], the Ru(II)-arene complexes have emerged as highly promising candidates. [11, 12, 13, 14].

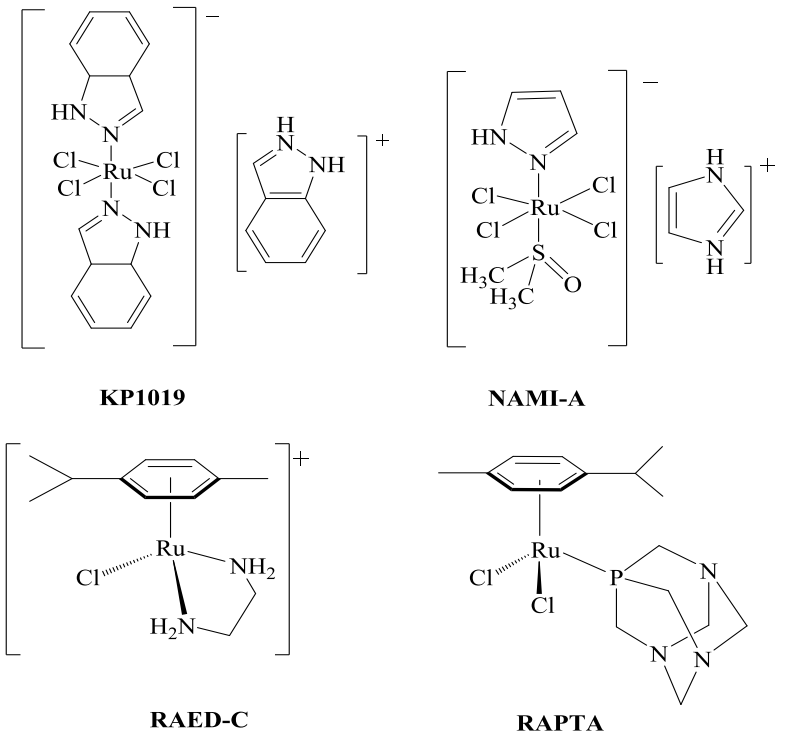

Figure 2: Complexes KP1019, NAMI-A, RAED-C, and RAPTA

RAPTA-C ([Ru(η^6-*p*-cymene)Cl_2(pta)]; pta = 1, 3, 5-triaza-7-phosphaadamantane) is a ruthenium-arene complex with a very hydrophobic aromatic benzene core, which prevents the oxidation of Ru(II) and due to its lipophilicity enhances entering to cells. RAED-C ([Ru(η^6-*p*-cymene)Cl(en)]; en = ethylenediamine) unlike RAPTA-C (Figure 2) reacts with the DNA component of chromatin in the cell, and shows high antitumor activity against primary cancer. Although the structural similarity with RAPTA-C is noticeable, the mechanism of cytotoxicity is quite different [15].

Thiourea and its derivatives have various applications due to different atoms included in their functional group, such as antiviral [16], herbicidal [17], anti-inflammatory [18] and fungicidal properties [19]. Bearing in mind problems with current metal drugs above described in combination with fact that requirements for safer, new and more active drugs are higher through years, specially taking into account the potential of the combination of a Ru-arene complex with thiourea derivatives as ligands, we have decided to conduct research for new metal-based anticancer candidates. The structure and chemical properties of metal complexes with derivatives of thiourea as ligands have been studied in recent years [20]. Derivatives of thiourea have more than one potential atom for coordination, and this ability mark them as good ligands in synthesis of complexes, as they can act as monodentate, bidentate or polydentate ligands coordinated through oxygen, nitrogen and sulfur atoms [21, 22]. There are many papers that document great anticancer and antimicrobial activity of this type of complexes [23, 24]. In addition to antimicrobial and cytotoxic activity, these compounds and complexes also exert various activities for instance antifungal, antithyroid, rodenticidal, insecticidal, herbicidal and other activities and properties [25, 26].

Synthetized Ru-arene complexes with thiourea derivatives as ligands are susceptible for additional exploration regarding therapeutic activities like antithyroid, antimicrobial, anticancer, even as

solution for tuberculosis treatment, as well as sensors and other optical solutions [27], and it can unquestionably bring beneficial to different areas, especially in medicine. Synthetized complexes are tested and evaluated by their cytotoxicity against HeLa cells and antimicrobial activity against several bacterial strains and yeast. By X-ray diffraction analysis, a formation of four member ring between thiourea based ligand and ruthenium metal center was revealed, as evidence that one ligand can have two binding modes in the same complex, as already reported in literature [22].

2. Experimental

2.1. Materials

All chemicals which were used for synthesis and testing antimicrobial and cytotoxic activity were of reagent-grade quality or higher, obtained from commercial suppliers (Sigma Aldrich) and were used without further purification. Solvents were used as received or dried over molecular sieves. $RuCl_3$ was purchased from I^2CNS.

2.2. Instrumental and methods

2.2.1. 1H and 13C NMR Spectroscopy

^1H and ^{13}C NMR spectra were recorded in deuterated solvents on a Bruker Ascend 400 (1H: 400 MHz, ^{13}C: 100.6 MHz), MHz spectrometer at room temperature internally referenced to TMS (tetramethylsilane). The chemical shifts, δ, are reported in ppm (parts per million), and coupling constants (*J*) in Hertz. The residual solvent peaks have been used as an internal reference. The abbreviations for the peak multiplicities are as follows: s (singlet), d (doublet), dd (doublet of doublets), t (triplet), q (quartet), m (multiplet), and br (broad).

2.2.2. ESI Mass and IR spectroscopy, elemental analysis

ESI (electrospray ionization) mass spectra were recorded on a LTQ Orbitrap XL using direct injection of the complex solution in methanol. Infrared spectra were recorded on a Nicolet 6700 FT-IR spectrometer using the ATR (attenuated total reflection) technique. Elemental analysis was carried out with Elemental Vario EL III microanalyser

2.2.3. Antimicrobial activity

Antimicrobial activity was tested by broth microdilution method according to guidelines of Clinical and Laboratory Standards Institute (CLSI) [28]. Minimum inhibitory concentrations (MIC) were determined as the lowest concentrations of tested chemical compounds that inhibited visible growth of microorganisms. Antimicrobial assay was carried out in 96-well polystyrene microtiter plates by using serial dilutions of the tested compounds (62.5-1000 µg/mL) dissolved in DMSO and further diluted in Mueller-Hinton broth for the bacterial strains and in Sabouraud dextrose broth for *Candida albicans.* Final concentration of DMSO in each well was 1%. The bacterial strains were previously prepared by incubating for 24 h at 35°C on Mueller-Hinton agar and for *Candida albicans* on Sabouraud dextrose agar. Fresh overnight cultures were suspended into sterile physiological saline (0.9% w/w NaCl) and adjusted to 0.5 McFarland standard which is approximately 2 x 10^8 CFU/mL (colony-forming unit/mL). The bacterial suspensions were further diluted in Mueller-Hinton broth to a final suspension with 1 x 10^6 CFU/ml and yeast was diluted in Sabouraud dextrose broth to a final suspension with 1 x 10^7 CFU/ml. 100 µl of each analyzed compound (complexes and ligands) and bacterial suspension were added in each well. To the bacterial suspensions 2, 3, 5-triphenyltetrazolium chloride (TTC) (Sigma-Aldrich, USA) was added as growth indicator. The final concentration of TTC after inoculation was 0.05%. Test compound stock solutions were prepared several minutes before they were used for testing.

Clinical Candida spp. strains were procured from BeoLab laboratories and Clinical-Hospital Centre Dragiša Mišović from Belgrade. Candida spp. strains identifications were managed using VITEK-2 system with YST ID cards. The MIC results were determined by visual method and interpreted after incubation of plates for 24 h at 35°C. Each test (included clinical isolates) was repeated three times, and all of the MIC determinations were performed in duplicate, with two positive growth controls included (wells containing only the microorganisms in the broth).

2.2.4. Cytotoxic activity

Cytotoxic activity of complexes and ligands were tested against cervix adenocarcinoma cell line (HeLa) with the aim of determining *in vitro* cytotoxic activity. The stock solutions of three investigated complexes and three ligands were dissolved in DMSO (Sigma-Aldrich, St. Louis, MO, USA) at the concentrations of 10 mM. Working concentrations were diluted by culture nutrient medium RPMI-1640 (Sigma-Aldrich, St. Louis, MO, USA) supplemented with 10% fetal bovine serum, 2 mM L-glutamine, and 1% penicillin-streptomycin (Sigma). HeLa cells were maintained in complete RPMI-1640 medium at 37 °C in humidified atmosphere with 5% CO_2 and seeded at a density of 2×10^3 cells/well in 96-well flat-bottomed microtitre plate. After twenty-four hours, cells were treated with different concentrations of investigated complexes and related ligands. Control cells were grown into the culture medium only. The final concentrations of treatments used in experiments were in the range of 12.5 μM to 200 μM (12.5, 25, 50, 100 and 200 μM). As a positive control we used cisplatin with the final concentrations of 3.125, 6.25, 12.5, 25, and 50 μM. The final concentration of DMSO solvent never exceeded 0.5 %, which is a non-toxic concentration for the cells. Culture medium without cells with different concentrations of complexes and ligands was used as blank. Experiments were set up in triplicate. The viability of cells was determined by micro culture tetrazolium test (MTT) as described previously [29]. After

72 hours of treatment with complexes and ligands, 10 µL of MTT solution (3-(4,5-dimethylthiazol-2-yl)-2,5-dyphenyl tetrazolium bromide) (5 mg/mL) was added to each well. After 4 hours of incubation, the product of the conversion of MTT dye by viable cells, formazan, was extracted by adding 100 µL of 10% SDS (100g/L sodium dodecyl sulfate) into the wells. On the next day, the intensity of the absorbance was measured at 570 nm using Multiskan EX reader (Thermo Labsystems Beverly, MA, USA), and it represented the number of viable cells in each well.

2.2.5. X-Ray spectroscopy

The X-ray intensity data were measured on Bruker D8 Venture diffractometer equipped with multilayer monochromator, Mo K/α INCOATEC micro focus sealed tube and Oxford cooling system. The structure was solved by direct methods. Non-hydrogen atoms were refined with *anisotropic displacement parameters*. Hydrogen atoms were inserted at calculated positions and refined with riding model. The following software was used: *Bruker SAINT* software package [30] using a narrow-frame algorithm for frame integration, *SADABS* [31] for absorption correction, *OLEX2* [32] for structure solution, refinement, molecular diagrams and graphical user-interface, Shelxle [33] for refinement and graphical user-interface *SHELXS-2015* [34] for structure solution, *SHELXL-2015* [35] for refinement, Platon [36] for symmetry check. Experimental data and CCDC-Codes Experimental data (Available online: http://www.ccdc.cam.ac.uk/conts/retrieving.html) can be found in Table S1. Crystal data, data collection parameters, and structure refinement details are given in Tables 1 and 2. Crystal structure is visualized in Figures 3 and 5.

2.2.6. Electrical Conductivity (EC)

Electrical conductivities of complexes were measured on Crison MultiMeter MM41 conductometer. EC measurements were performed using 1 mM solutions of the complexes in acetonitrile and acetone as solvents at 25 ˚C.

2.3.1. Synthesis of ligands

All three ligands N-([4-methoxyphenyl]carbamothioyl)benzamide (L^1), 4-(3-benzoylthioureido)benzoic acid (L^2) and methyl 4-(3-benzoylthioureido)benzoate (L^3) were synthesized according to a slightly modified published procedure [37]. Potassium thiocyanate has been condensed with benzoyl chloride resulting of forming benzoyl-isothiocyanates and reacting with primary amines in the next phase (Scheme 1). The ruthenium dimer $[(\eta^6\text{-}p\text{- cymene})RuCl_2]_2$ was prepared according to a published procedure [38].

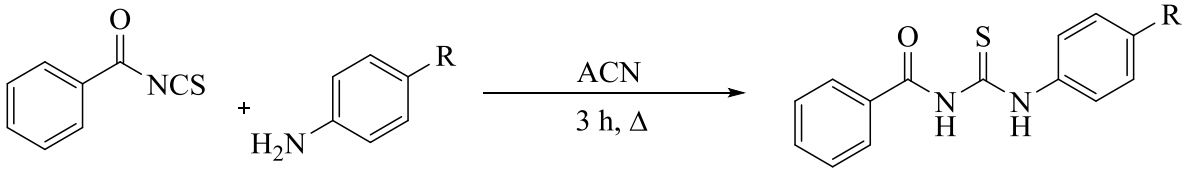

R_1 = OMe (**L1**)
R_2 = COOH (**L2**)
R_3 = COOMe (**L3**)

Sheme 1*:* Synthesis of aromatic derivatives of thiourea

*2.3.2. General synthesis of the complexes **C1-C3***

To a suspension of $[(\eta^6\text{-}p\text{-cymene})RuCl_2]_2$ (0.053 mmol; 1 eq) in absolute ethanol (toluene in case of **C2**) (8 ml) was added dropwise a solution of ligand (L^1 - L^3; 0.105 mmol; 2 eq) in absolute ethanol (10 ml) with constant stirring. The mixture was stirred at 60 ºC for 4 h. During this time

orange precipitate of complex was formed. Precipitate was filtered, and washed with cold ethanol (10 ml) and diethyl-ether (10 ml) and dried in vacuo.

[Ru(η^6-p-cymene)(L^1)Cl_2] ***(C1)***

Yield: 48 mg (75%). Elemental analysis, calculated for $C_{25}H_{28}Cl_2N_2O_2RuS$: C 50.68; H 4.76; N 4.73; S 5.41. Found: C 50.89; H 4.66; N 4.50; S 5.15. IR (ATR, cm^{-1}): 3133 (m), 3028 (m), 2961 (m), 1656 (s), 1526 (s), 1271 (m), 1168 (m). ^{1}H NMR (400 MHz, DMSO-d6) δ 12.79 (s, 1H), 11.68 (s, 1H), 8.01 (d, *J* = 8.8 Hz, 4H), 7.92 (m, 2H), 7.68 (m, 1H), 7.55 (m, 2H), 5.78 (m, 4H), 2.84 (dt, *J* = 13.8, 6.9 Hz, 1H), 2.59 (s, 3H), 2.09 (s, 3H), 1.19 (s, 6H). ^{13}C NMR (101 MHz, DMSO-d6) δ 197.3, 179.4, 168.6, 142.6, 134.6, 133.7, 132.5, 129.4, 129.2, 128.9, 123.9, 106.8, 100.5, 86.8, 85.5, 30.4, 27.1, 21.9, 18.3. ESI-MS: m/z 521.08 ($[M\text{-}Cl\text{-}HCL]^+$).

[Ru(η^6-p-cymene)(L^2)Cl_2] ***(C2)***

Yield: 32 mg (48%). Elemental analysis, calculated for $C_{25}H_{26}Cl_2N_2O_3RuS$: C 49.51; H 4.32; N 4.62; S 5.29. Found: C 49.82; H 4.29; N 4.63; S 4.85. IR (ATR, cm^{-1}): 3054 (m), 2971 (m), 1689 (s), 1537 (s), 1267 (m), 1172 (m). ^{1}H NMR (400 MHz, DMSO-d6) δ 12.77 (s, 1H), 11.64 (s, 1H), 10.52 (s, 1H) 7.98 (m, 4H), 7.91 (m, 2H), 7.67 (m, 1H), 7.55 (m, 2H), 5.79 (d, J = 11.9 Hz, 4H), 2.84 (s, 1H), 2.09 (s, 3H), 1.20 (s, 6H). ^{13}C NMR (101 MHz, DMSO-d6) δ 179.4, 168.6, 167.1, 142.4, 133.6, 132.5, 130.6, 130.4, 129.2, 128.9, 128.5, 128.2, 123.9, 119.9, 106.8, 100.5, 86.8, 85.9, 65.3, 30.4, 21.9, 18.3, 15.6**.** ESI-MS: m/z 535.06 ($[M\text{-}Cl\text{-}HCL]^+$).

[Ru(η^6-p-cymene)(L^3)Cl_2] ***(C3)***

Yield: 42 mg (70%). Elemental analysis, calculated for $C_{26}H_{28}Cl_2N_2O_3RuS$: C 50.32; H 4.55; N 4.51; S 5.17. Found: C 50.54; H 4.62; N 4.49; S 5.04. IR (ATR, cm^{-1}): 2963 (m), 1671 (s), 1544 (s), 1277 (m), 1170 (m). ^{1}H NMR (400 MHz, DMSO-d6) δ 12.46 (s, 1H), 11.50 (s, 1H), 7.98 (d,

J = 7.6 Hz, 2H), 7.66 (m, *J* = 7.3 Hz, 1H), 7.55 (dd, *J* = 13.5, 8.0 Hz, 4H), 6.98 (m, *J* = 8.7 Hz, 2H), 5.80 (m, *J* = 17.4, 6.0 Hz, 4H), 3.78 (s, 3H), 2.84 (dt, *J* = 13.6, 6.9 Hz, 1H), 2.05 (d, *J* = 33.1 Hz, 3H), 1.18 (m, 6H). ^{13}C NMR (101 MHz, DMSO-d6) δ 179.6, 168.7, 157.9, 133.5, 132.6, 131.3, 129.1, 128.9, 126.4, 114.3, 106.8, 100.5, 86.8, 85.9, 55.8, 21.9, 18.3. ESI-MS: m/z 549.07 ([M-Cl-HCL]$^{+}$).

3. Results and discussion

3.1. Synthesis and characterization of Ru complexes

All three complexes were synthetized using a suspension of $[(\eta^6\text{-p-cymene})RuCl_2]_2$ in absolute ethanol or toluene with dropwise addition of previously synthesized ligand dissolved in absolute ethanol with constant stirring for several hours (Scheme 2). During the reaction period, orange precipitates of complexes were formed. Precipitates were filtered, and washed with cold ethanol and diethyl-ether and dried in vacuo. The products were isolated in a moderate good and good yields. Complexes were characterized by ^{1}H and ^{13}C NMR, IR, mass spectrometry, and in the case of **C1** the structure has been determined by X-ray analysis. In the ^{1}H and ^{13}C NMR spectra of the complexes, all hydrogen and carbon atoms appear at chemical shifts expected for such types of compounds. Collected data suggest monodentate coordination of ligands, likely due to formation of kinetic reaction products. Similar molecules as ligands used in this work, 1-acyl-thiourea derivatives, tend to form intramolecular N-H⋯O=C hydrogen bond [39, 40]. Formation of intramolecular hydrogen bond resultes making of six membered ring in molecule. Distorsion of molecule allows right conformation for coordination of S and N atoms to the ruthenium center. This allows formation of thermo-dynamic product of the complex, isolated as monocrystal. Compex **C1** showed in X-ray analysis piano-stool geometry with a coordinated chloride ligand

and four-membered ring through N and S bidentate coordinaton of derivative of benzoylthiourea. Complexes showed very good solubility in dimethyl sulfoxide, good in acetonitrile and acetone, but moderate solubility in ethanol and methanol.

IR spectra of ligands and corresponding complexes revealed all expected bands of interest- ν(N-H), ν(C=O), ν(C-N), ν(C-O), ν(C=S), ν(C=C)$_{ar}$ and ν(O-H). Ligand bands of ν(N-H) can be identified in the range of 3262-3225 cm^{-1}. The strong ligand absorption bands of ν(C=S), ν(C-N), ν(C=O) and ν(C=C)$_{ar}$ were observed in range of 1160– 1150 cm^{-1}, 1269–1259 cm^{-1}, 1689–1667 cm^{-1} and 1535–1522 cm^{-1}, respectively. Ligand L^{1} as a derivative of benzoic acid has ν(O-H) absorption band at 3004 cm^{-1}. In addition, the existence of absorption bands for C=S can be observed in the range of 705-687 cm^{-1} which it highly indicated that all ligands are indeed thiourea derivatives. Upon coordination absorption bands of relevant groups in the complexes were slightly shifted to the higher values. Bands of interest for the complexes are the same bands as for ligands ν(N-H), ν(C=O), ν(C-N), ν(C=S), ν(C=C)$_{ar}$ and ν(O-H). They were found in range of 3207– 2963 cm^{-1}, 1689–1656 cm^{-1}, 1277–1267 cm^{-1} 1172–1163 cm^{-1}, 1535–1522 cm^{-1}, and 2971 cm^{-1}, respectively. Existence of absorption bands for C=S can be observed in the range of 755-701 cm^{-1} and indicate that all complexes are indeed thiourea derivatives.

The ^{1}H NMR spectra contain a characteristic pattern for the *p*-cymene moiety. A methyl group singlet is observed at 2.09 ppm, the resonance signal of –CH(CH$_3$)$_2$ appears as a multiplet in a range of 2.82-2.85 ppm and -CH(CH$_3$)$_2$ as a doublet in range of 1.09-1.19 ppm. The signals of the arene ring protons were found in a range of 5.77-5.83 ppm. Aromatic region of the ^{1}H-NMR spectra of the complexes **C1**-**C3** was found in a range of 7.51-8.03 ppm. Interestingly, that protons from two N-H groups in thiourea are at very high chemical shifts of 11.68-11.5 ppm and 12.79-12.46 ppm, suggesting significant acidity. Change in proton shifts are noticeable from **L^{1}** to **C1** where aromatic protons have different pattern. Also N-H group protons in this case, were shifted

from 9.1 ppm and 12.5 ppm in the free ligand to 11.7 ppm and 12.8 ppm in the complex, respectively. Similar observation of different pattern is visible in aromatic protons of free ligand **L^3** and corresponding complex, with the less shift change in N-H group protons (stacked spectra in SI). In the case of **C2,** the difference in ligand and complex proton shifts are much less obvious. The ^{13}C NMR spectra of synthesized complexes didn't suffer significant changes comparing to spectra of uncoordinated ligand except in case of **C1** and **C3** in thiourea group. Chemical shifts correspond to the already described complexes of this type. The ^{13}C-NMR spectra display chemical shift at 18.3 ppm from the methyl group attached to the *p*-cymene moiety, 21.9 ppm from $–CH(CH_3)_2$, while the chemical shift at 30.4 ppm is due to the $CH(CH_3)_2$ group. The aromatic carbon atoms from cymene display chemical shifts within range of 100.5–142.6 ppm. Carbon atoms signals from double bond C=S are located in complexes around 179 ppm, and carbon atom chemical shifts from C=O bond in range 167.1-168.7 ppm. Most changes in this region is visible of thiourea group of complex **C1** and **C3**.

Mass spectra of the complexes were recorded in a positive ion mode. Molecular ions were detected at 521.8 ($[M\text{-}Cl\text{ -}HCL]^+$) for **C1**, 535.06 ($[M\text{-}Cl\text{-}HCL]^+$) for **C2**, and 549.07 ($[M\text{-}Cl\text{-}HCL]^+$) for **C3**.

Acetonitrile has been used as complex solvent bearing in mind that acetonitrile possesses high dielectric constant and low viscosity relative to other solvents which are preferred for conductivity measurements. Conductivity analysis with acetone as complex solvent were performed as well. Conductivity values for 1 mM solutions of **C1** in acetonitrile and acetone are 15.49 and 0.53 $\Omega^{-1}cm^2mol^{-1}$, respectively, while the conductivity values for **C2** are 17.79 and 3.26, respectively. Result for **C3** in acetonitrile is 10.92 while result in acetone is 1.36 $\Omega^{-1}cm^2mol^{-1}$. Based on the very low values and literature data [41] we concluded that all complexes are a neutral species, as

expected values for 1:1 electrolyte type in acetone and acetonitrile are in range 100 - 140, and 120 - 160 $\Omega^{-1}cm^2mol^{-1}$, respectively.

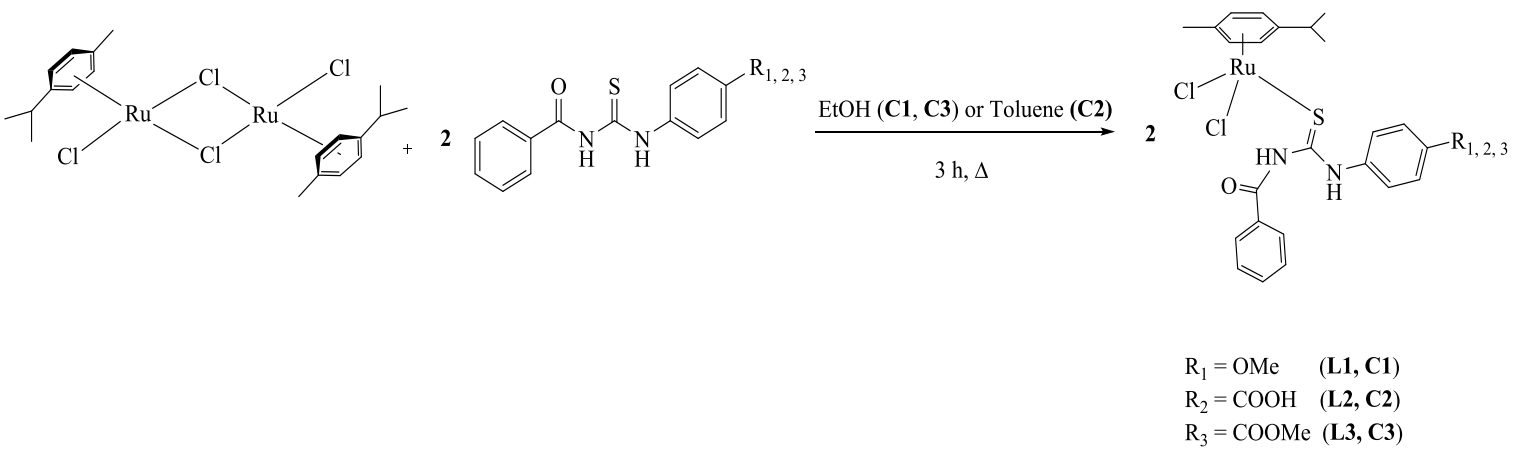

Scheme 2: Synthesis of **C1-C3**

3.2. X-ray analysis

In contrast to the data obtained by NMR and elemental analysis, coordination of thiourea ligand has changed from monodentate to bidentate of isolated crystal, corresponding to complex **C1**. Similar findings are already reported in literature [22, 42]. Piano-stool geometry for the compound consists of coordinated chlorido ligand and four-membered ring through N and S bidentate coordinaton of derivative of benzoylthiourea. The results of X-ray diffraction studies are shown in Figure 4. Geometrical environment around ruthenium atom has the typical "three leg piano-stool'' geometry, which is common for a large number of ruthenium(II) arene species. Although it is well known that the most stable chelate ring is is a five-membered one, in a case of ligands used in this work, formation of five-membered ring is not possible.

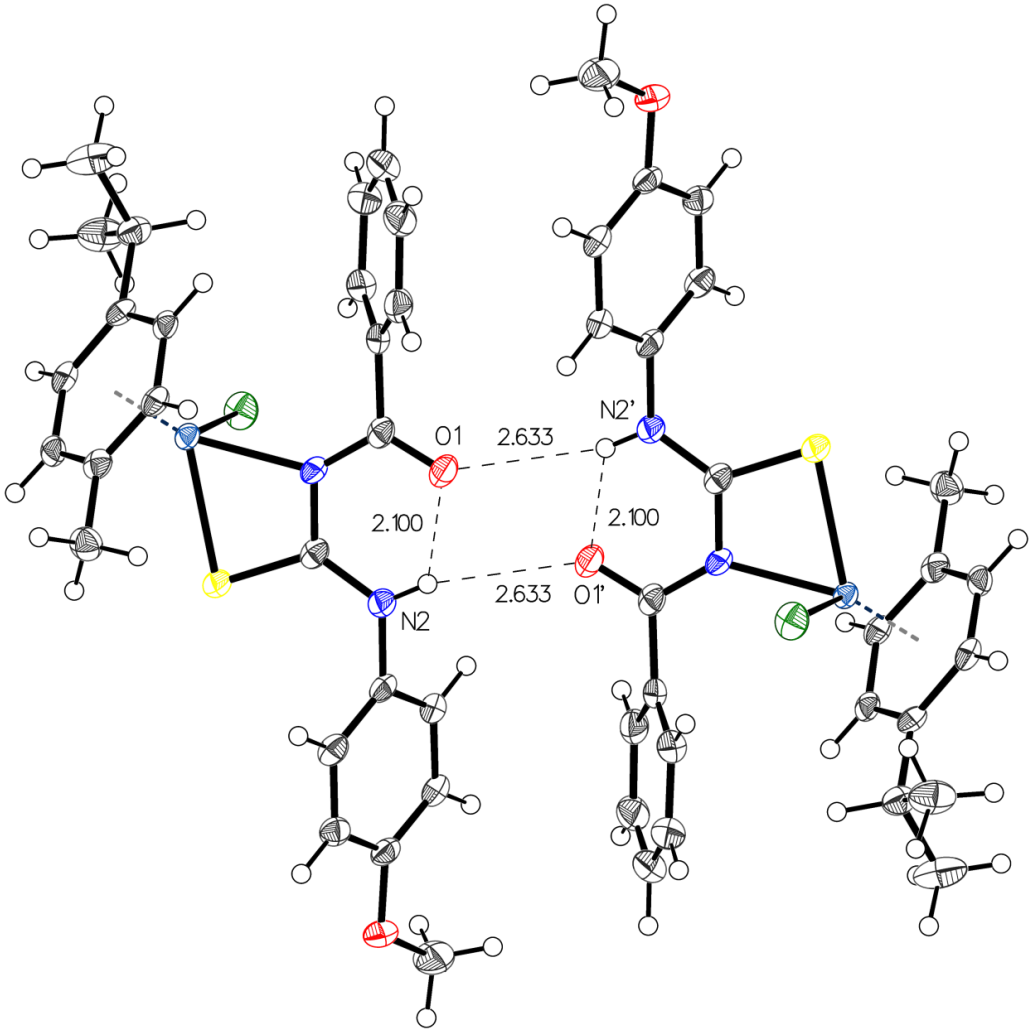

Figure 3. Two molecules of **C1** associated into a centrosymmetric dimer via two bifurcated hydrogen bonds

In Figure 3, two different hydrogen bonds could be detected, one intramolecular (N2-H2…O1), one intermolecular (N2-H2…O1'). With the help of the intramolecular hydrogen bond a six membered pseudo ring is formed. Those rings contribute to the stabilization of the complex [43]. In this context Platon detects one short interaction between O1 and O1' (2.79Å). Details are presented in Table 1 and Figure 4.

Table 1: Specified hydrogen bonds (with esds except fixed and riding H)

D-H	H...A	D...A	<(DHA)	
0.82	2.10	2.662(3)	125	N2-H2...O1
0.82	2.63	3.429(3)	163	N2-H2...O1'

' … [-x, -y+1, -z]

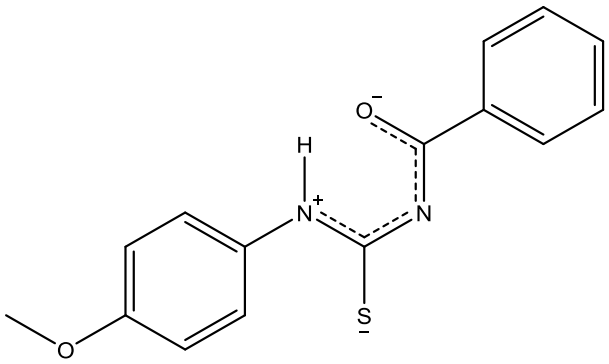

Figure 4. Mono-anion L1

Table 2: Bond lengths in the four-membered ring on the Ru centre.

	Ru1-S1	S1-C1	C1-N1	N1-Ru1	CCDC Codes
	Å	Å	Å	Å	
C1	2.416(5)	1.714	1.365	2.138(3)	1959425
Hang Zhu et al.[44]	2.460(3)	1.708	1.324	2.209(6)	813250
	2.442(2)	1.727	1.331	2.207(6)	813250
Xi-Ying Wang et al.[45]	2.478(14)	1.729	1.317	2.109(4)	776948
Ai-Quan Jia et al.[46]	2.495(8)	1.714	1.315	2.164(2)	854737
Ai-Quan Jia et al.[47]	2.455(9)	1.722	1.320	2.165(2)	854738
Ai-Quan Jia et al.[48]	2.438(9)	1.720	1.312	2.158(3)	854739
M.Aitali et al.[49]	2.438(3)	1.730	1.343	2.097(8)	150372
	2.429(3)	1.724	1.311	2.094(8)	150372

Complex corresponding to **C1** is similar to all listed XRD results. We can classify the bond S1-C1 as single bond and C1-N1 as delocalised double bond which is in good accordance to the planar geometry along the bonds of L1 in the four membered ring, see Figure 4. Therefore, we can interpret L1 as mono-anion. The Ru1-S1 bond seems to be short in relation to the listed results but M. Aitali et al. with identical ligands of chlorido and *p*-cymene as in **C1** shows also shorter bond length. Also listed experiments were performed at room temperature, whereas **C1** was recorded at 100K. The centre of gravity ring distance of the *p*-cymene is 1.6698Å. Finally, the ring slippage of the *p*-cymene with 0.036Å is detected and is not uncommon.

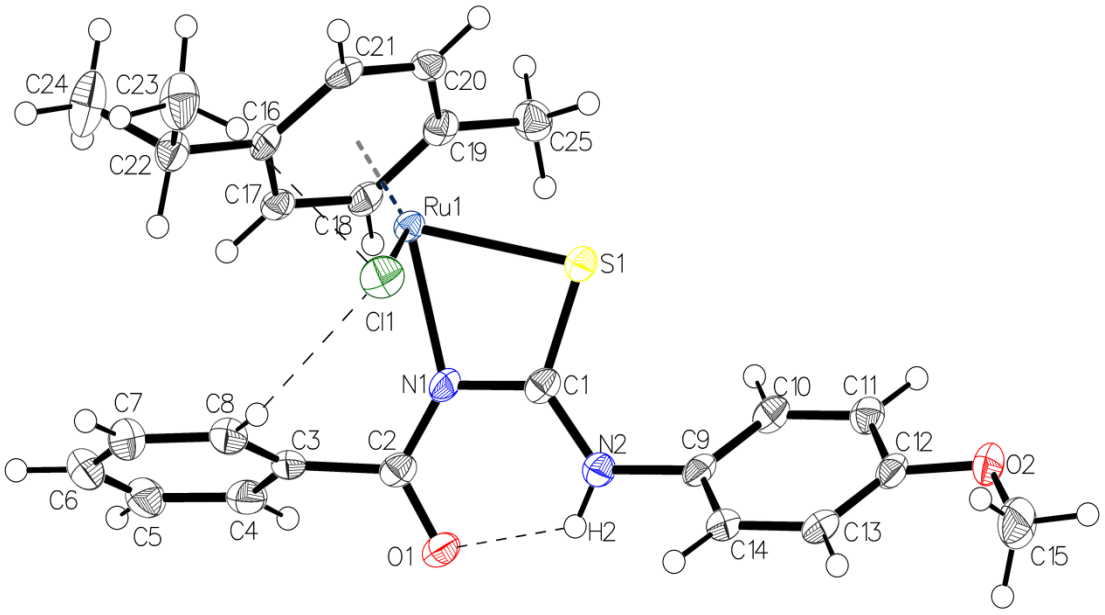

Figure 5: X-ray structure of complex **C1**

3.3. Antimicrobial activity

Growing need for efficient antibacterial and antifungal agent is caused by rapid emergence of multi resistant bacterial strains developing resistance [50, 51, 52, 53]. For the first time, the antimicrobial

activity of synthesized complexes was investigated against nine bacterial strains: *Staphylococcus aureus* (ATCC 6538), *Staphylococcus epidermidis* (ATCC 1228), *Enterococcus faecalis* (ATCC 29212), *Bacillus subtilis* (ATCC 6633), *MRSA* (clinical isolate), *Escherichia coli* (ATCC 10536), *Klebsiella pneumoniae* (NCIMB 9111), *Salmonella abony* (ATCC 6017), *Pseudomonas aeruginosa* (ATCC 27853) and one strain of yeast *Candida albicans* (ATCC 24433).

Results indicate that the investigated complexes and related ligands were less active than the standard antimicrobial and antifungal drugs (Table S6). In most antimicrobial assays complexes expressed better antimicrobial and antifungal activity than their related ligands. All complexes expressed low to moderate antimicrobial activity. Complexes **C1** and **C3** expressed significant antimicrobial activity against *C. albicans* (MIC=62.5 µg/mL for both complexes) among tested. For that reason, we tested clinical Candida spp. strain isolates as well. The results are shown in Table 3. Complex **C1** expressed higher antimicrobial activity then other complexes and ligands, especially on systemic infection isolates (MIC ranged between 62.5-500 µg/mL).

Table 3: Antimicrobial activity of complexes and theirs related ligands against Candida spp. clinical strain isolates (MIC values are given in µg/ml)

	MIC (µg/ml)							
Type of infection	Type of sample	Strain number	**Ligand**			**Complex**		
			L^1	**L^2**	**L^3**	**C1**	**C2**	**C3**
Local infections strains	vaginal swab	2	>1000	>1000	>1000	250	>1000	1000
	vaginal swab	3	>1000	>1000	>1000	500	>1000	1000
	vaginal swab	7	>1000	>1000	>1000	250	>1000	1000
	cervical swab	8	500	n.t.	125	1000	>1000	>1000
	vaginal swab	20	250	n.t.	1000	1000	>1000	>1000

	cervical swab	21	>1000	n.t.	>1000	1000	>1000	>1000
	vaginal swab	22	>1000	1000	>1000	**62,5**	125	**62,5**
Systemic infections strains	sputum	670	>1000	>1000	500	125	1000	1000
	sputum	712	1000	>1000	>1000	500	1000	>1000
	sputum	719	1000	>1000	>1000	**62,5**	>1000	>1000
	sputum	791	250	>1000	1000	**62,5**	>1000	1000
	sputum	805	125	500	500	250	1000	250
	tracheal swab	826	>1000	>1000	>1000	250	>1000	1000
	Chemoculture	1067	62,5	n.t.	>1000	250	>1000	>1000

*n.t- not tested

3.4.1. Cytotoxic activity

The anticancer activity of investigated ruthenium complexes and related ligands was examined against human cervix adenocarcinoma (HeLa) cell line by MTT test incubated for 72h with different concentrations of complexes or ligands. The positive control was cisplatin. The results for IC_{50} concentrations are shown in Table 4.

Table 4: Concentrations of compounds that induced a 50% decrease in HeLa cell survival rate expressed as IC_{50} (μM).

Class of compound	Compounds	IC_{50}(μM)
		HeLa
Complexes		

	C1	29.7 ± 0.9
	C2	52.4 ± 4.0
	C3	32.4 ± 3.2
Ligands	L^1	46.2 ± 0.5
	L^2	56.6 ± 6.9
	L^3	69.6 ± 7.3
Positive control	Cisplatin	4.6 ± 0.1

IC_{50} concentrations of ligands L^1, L^2 and L^3 and complexes **C1**, **C2** and **C3** were ranging from 29.7 to 69.6 μM. Comparative dose-response survival curves of HeLa cells treated with different concentrations of synthesized ligands and their complexes are presented on graphs in Fig. 6. Complexes **C1** and **C3** showed significant lower IC_{50} values than IC_{50} values of ligands L^1 and L^3, respectively. The most efficient anticancer activity had complex **C1** with IC_{50} value 29,7 μM but the biggest difference in IC_{50} values and anticancer activity compared with its ligand showed complex **C3**. Complex **C2** and related ligand L^2 had the similar values of IC_{50} concentration Graphs are showing that complexes **C1**, **C2** and **C3** have better cytotoxic activity than ligands L^1, L^2 and L^3 at concentrations higher than IC_{50} concentrations. Also, this trend of cytotoxicity activity can also be explained by differences in lipophilicity of the complex, where complex **C1** is the most lipophilic, and **C2** is the most polar. All examined compounds had higher IC_{50} values when comparing with positive control, cisplatin.

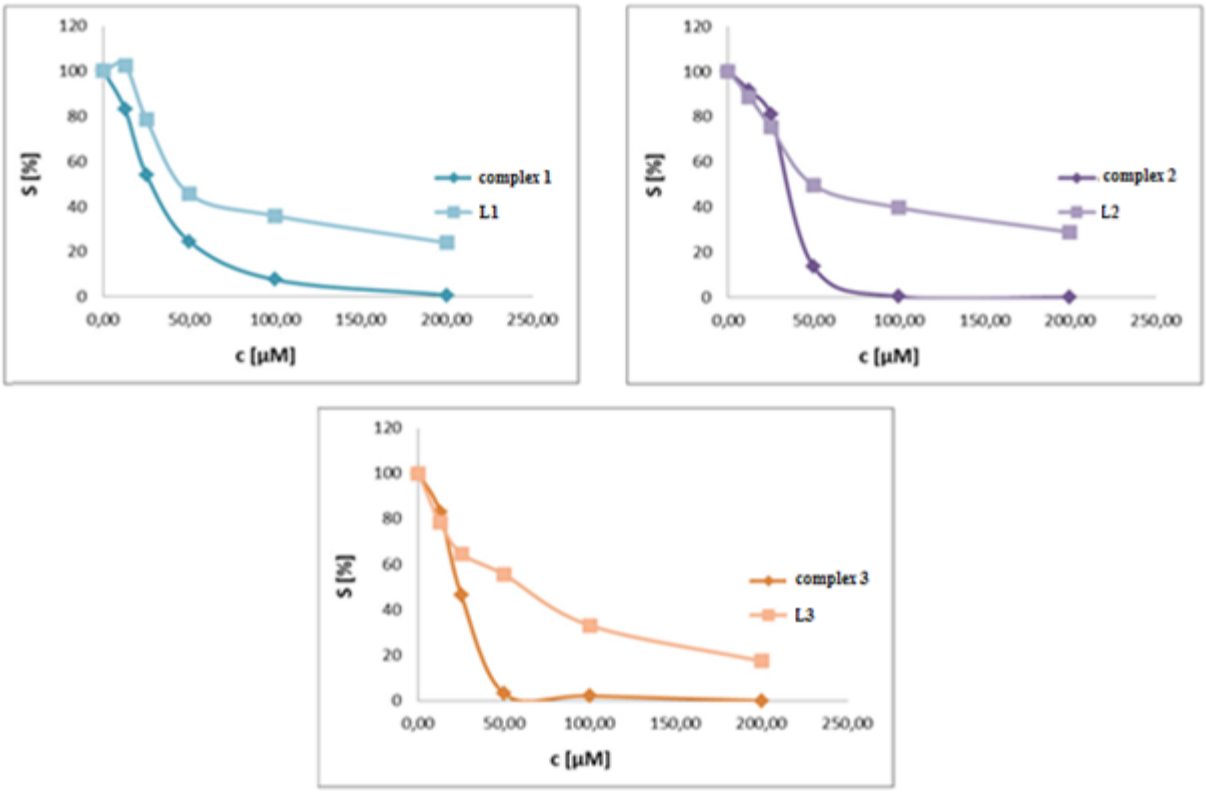

Figure 6: The survival of HeLa cells incubated for 72h with different concentrations of synthesized ligands and Ru complexes

4. Conclusion

In this study three half-sandwich ruthenium complexes have been synthesized and characterized with several instrumental methods and evaluated for antimicrobial and cytotoxic activity. All complexes were isolated as neutral complexes with monodentate coordination of thiourea ligand. X-ray structure analysis revealed the piano stool geometry around ruthenium center with the formation of a four-membered ring between ruthenium ion and sulfur and nitrogen atoms from ligand. Antimicrobial activity has been evaluated against nine Gram-positive and Gram-negative bacterial strains and one yeast - *Candida albicans*. Complexes **C1** and **C3** exerted moderate antibacterial activity against *S. aureus* (MIC=500 µg/mL for complex **C1** and MIC=250 µg/mL

for complex **C3**) and the best antimicrobial activity against *C. albicans* (MIC=62.5 µg/mL for both complexes). At the same time, complex **C1** expressed higher antimicrobial activity against Candida spp. clinical isolates then other complexes and ligands, especially on systemic infection isolates (MIC ranged between 62,5-500 µg/mL). Corresponding ligands had MIC values ranged from 250 to 1000 µg/mL in the most analyzed examples. The anticancer activity of investigated ruthenium complexes and related ligands was examined against human cervix adenocarcinoma (HeLa) cell line. Compounds showed moderate anticancer activity, with complex **C1** being the most effective one. All compounds had less efficient cytotoxic activity against HeLa cells in comparison to cisplatin. In the expanding field of the rational drug discovery, ruthenium complexes represent promising class of small molecules that can be optimized to more specifically target tumor cells. Future study will be focused toward synthetizing complexes with higher activity and selectivity.

Abbreviations:

MIC- Minimal inhibitory concentration

DNA-Deoxyribonucleic acid

KP1019 – indazolium-trans-tetrachlorobis(1H-indazole)ruthenate(III)

KP1339 – sodium-trans-tetrachlorobis(1H-indazole)ruthenate(III)

NAMI – sodium-trans-imidazoledimethylsulfoxidetetrachlororuthenate(III)

HeLa- human cervix adenocarcinoma cells

FemX- human melanoma cells

A549- lung adenocarcinoma cells

MRC-5- human fetal fibroblast cells

ESI- Electrospray ionization

DFT- Density Functional Theory

CLSI- Clinical and Laboratory Standards Institute

TTC- 2, 3, 5-triphenyltetrazolium chloride

RPMI-1640- Roswell Park Memorial Institute

DMSO- dimethyl sulfoxide

DMSO-d6 – deuterated dimethyl sulfoxide

L1- *N*-((4-methoxyphenyl)carbamothioil)benzamide

L2- 4-(3-benzoylthioureido)benzoic acid

L3- Methyl-4-(3-benzoyltioureido)-benzoate

NAG- *N*-acetylglucosamine

NAM- *N*-acetylmuramic acid

MTT 3-(4,5-dimethylthiazol-2-yl)-2,5-diphenyltetrazolium bromide

IC_{50}-Inhibitory concentration

Acknowledgements

This work was supported by the Ministry of Education, Science and Technological Development of Republic of Serbia Contract number: 451-03-68/2020-14/200288.

References

[1] https://www.who.int/en/news-room/fact-sheets/detail/noncommunicable-diseases

[2] R. Canetta, K. Bragman, L. Smaldone, M. Rozencweig, Cancer Treat. Rev. 15 (1988) 17.

[3] J. P. Caussanel, F. Levi, S. Brienza, J. L. Misset, M. Itzhaki, R. Adam, G. Milano, B. Hecquet, G. Mathe, J. Natl. Cancer Inst., 82 (1990) 1046.

[4] N. Muhammad, Z. Guo, Curr. Opin. Chem. Biol. 19 (2014) 144–153.

[5] A. Bergamo, C. Gaiddon, J. H. Schellens, J. H. Beijnen, G. Sava, J. Inorg. Biochem. 106 (2012) 90–99.

[6] R. Trondl, P. Heffeter, C.R. Kowol, M.A. Jakupec,W. Berger, B.K. Keppler, Chem. Sci. 5 (2014) 2925–2932.

[7] S. Leijen, S. A. Burgers, P. Baas, D. Pluim, M. Tibben, E. van Werkhoven, E. Alessio, G. Sava, J. H. Beijnen, J. H. Schellens, Invest New Drugs. 33 (2015) 201-214.

[8] P. J. Dyson, G. Sava, Dalton Trans. 1 (2006) 1929-1933.

[9] C.G. Hartinger, S. Zorbas-Seifried, M. A. Jakupec, B. Kynast, H. Zorbas, B. K. Keppler, J. Inorg. Biochem. 100 (2006) 891-904.

[10] W. H. Ang, P. J. Dyson, Eur. J. Inorg. Chem. 20 (2006) 8153

[11] H.-K. Liu, P.J. Sadler, Acc. Chem. Res. 44 (2011) 349–359.

[12] W.M. Motswainyana, P.A. Ajibade, Adv. Chem. (2015) ID 859730.

[13] A. A. Nazarov, C. G. Hartinger, P. J. Dyson, J. Organomet. Chem. 751 (2014) 251-260.

[14] B. S. Murray, M. V. Babak, C. G. Hartinger, P. J. Dyson, Coord. Chem. Rev. 306 (2016) 86–114.

[15] A. Weiss, R. H. Berndsen, M. Dubois, C. Muller, R. Schibli, A. W. Griffioen, P. J. Dyson, P. Nowak Sliwinska, Chem. Sci. 5 (2014) 4742-4748.

[16] L. Qiao, J. Huang, W. Hu, Y. Zhang, J. J. Guo, W. L. Cao, K. H. Miao, B. F. Qin, J. R. Song, J. Mol. Struct. 1139 (2017) 149-159.

[17] B. Anna, S. Joanna, S. Karolina, N. Agnieszka, A. K. Ewa, S. Giuseppina, M. Silvia, B. Stefano, G. Gabriele, W. Małgorzata, S. Marta, Eur. J. Med. Chem. 101 (2015) 111.

[18] S. Sohail, R. Naghmana, G. J. Peter, H. Rizwan, H. B. Moazzam, Cent. Eur. J. Chem. 8 (2010) 550-558.

[19] L. Qiao, Y. Zhang, W. Hu, J. J. Guo, W. L. Cao, Z. M. Ding, Z. W. Guo, A. Fan, J. R. Song, J. Huang, J. Mol. Struct. 1141 (2017) 309–321.

[20] J. Akhtar, J. C. Bruce, M. A. Malik, K. R. Koch, M. Afzaal, P. O'Brien, Mater. Res. Soc. Symp. Proc. 1148E (2009) 1148.

[21] A. Rilak, R. Puchta, Ž. D. Bugarčić, Polyhedron 91 (2015) 73–83.

[22] B. N. Cunhaa, L. Colina-Vegas, A. M. Plutín, R. G. Silveira, J. Honorato, K. M. Oliveira, M. R. Cominetti, A. G. Ferreira, E. E. Castellano, A. A. Batista, J. Inorg. Biochem. 186 (2018) 147–156.

[23] A. Molter, S.Kathrein, B. Kircher, F. Mohr, Dalton Trans. 47 (2018) 5055-5064.

[24] R. S. Correa, K. M. de Oliveira, F. G. Delolo, A. Alvarez, R. Mocelo, A. M. Plutin, M. R. Cominetti, E. E. Castellano, A. A. Batista, J. Inorg. Biochem. 150 (2015) 63–71.

[25] M. M. Ghorab, M. S. Alsaid, M. S. A. El-Gaby, M. M. Elaasser, Y. M. Nissan, Chem Cent J. 11 (2017) 32.

[26] R.-Z. Huang, B. Zhang, X.-C. Huangb, G.-B. Lianga, J.-M. Qina, Y.-M. Pana, Z.-X. Liao, H.-S. Wang, RSC Adv. 7 (2017) 8866-8878

[27] R. K. Mohapatra, P. K. Das, M. K. Pradhan, M. M. El-Ajaily, D. Das, H.F. Salem, U. Mahanta, G. Badhei, P. K. Parhi, A. A. Maihub, Md. K.E-Zahan, Comment Inorg Chem 39 (2019) 127-187.

[28] Clinical and Laboratory Standardads Institute (CLSI) 2016. Performance standards for antimicrobial susceptibility testing, 26th Informational Supplement. Approved Standard. CLSI document M100S. Wayne, PA, USA

[29] I. Z. Matić, I. Aljančić, Ž. Žižak, V. Vajs, M. Jadranin, S. Milosavljević, Z. D. Juranić, BMC Complement. Altern. Med. 13 (2013) 36.

[30] Bruker SAINT v8.38B Copyright © 2005-2019 Bruker AXS

[31] Sheldrick, G. M. (1996). SADABS. University of Göttingen, Germany.

[32] O. V. Dolomanov, L. J. Bourhis, R. J. Gildea, J. A. K. Howard, H. Puschmann, OLEX2, J. Appl. Cryst. 42 (2009) 339-341.

[33] C. B. Huebschle, G. M. Sheldrick and B. Dittrich, ShelXle: a Qt graphical user interface for SHELXL, J. Appl. Cryst., 44 (2011) 1281-1284.

[34] G. M. Sheldrick, (2015). SHELXS v 2016/4 University of Göttingen, Germany.

[35] G. M. Sheldrick, (2015). SHELXL v 2016/4 University of Göttingen, Germany.

[36] A. L. Spek, Acta Cryst. D65 (2009) 148-155.

[37] T. O. Brito, A. X. Souza, Y. C. C. Mota, V. S. S. Morais, L. T. De Souza, A. de Fatima, F. Macedo Jr, L. V. Modolo, RSC Adv. 5 (2015) 44507.

[38] S.B. Jensen, S.J. Rodger, M.D. Spicer, J. Organomet. Chem. 556 (1998) 151–158.

[39] A. Saeed, A. Khurshid, J.P. Jasinski, C.G. Pozzi, A.C. Fantoni, M.F. Erben, Chem.

Phys. 431-432 (2014) 39–46.

[40] A. Saeed, U. Flörke, M.F. Erben, J. Sulfur Chem. 35 (2013) 318–355.

[41] W. J. Geary (1971) Coord. Chem. Rev. 81-122

[42] K.R. Koch, Coord. Chem. Rev. 216-217 (2001) 473–488.

[43] K. B. Wiberg, Angew. Chem. Int. Ed. 25 (1986) 312–322.

[44] Hang Zhu, Qing Ma, Ai-Quan Jia, Qun Chen, Wa-Hung Leung, Qian-Feng Zhang CCDC 813250: Experimental Crystal Structure Determination, 2013, DOI: 10.5517/ccw97w8

[45] Xi-Ying Wang, Hua-Tian Shi, Fang-Hui Wu, Qian-Feng Zhang CCDC 776948: Experimental Crystal Structure Determination, 2011, DOI: 10.5517/ccv2gv6.

[46] Ai-Quan Jia, Qing Ma, Qun Chen, Hua-Tian Shi, Wa-Hung Leung, Qian-Feng Zhang CCDC 854737: Experimental Crystal Structure Determination, 2012, DOI: 10.5517/ccxpf55.

[47] Ai-Quan Jia, Qing Ma, Qun Chen, Hua-Tian Shi, Wa-Hung Leung, Qian-Feng Zhang CCDC 854738: Experimental Crystal Structure Determination, 2012, DOI: 10.5517/ccxpf66.

[48] Ai-Quan Jia, Qing Ma, Qun Chen, Hua-Tian Shi, Wa-Hung Leung, Qian-Feng Zhang CCDC 854739: Experimental Crystal Structure Determination, 2012, DOI: 10.5517/ccxpf77.

[49] M. Aitali, M. Y. Ait Itto, A. Hasnaoui, A. Riahi, A. Karim, S. Garcia-Granda, A. Gutierrez-Rodriguez CCDC 150372: Experimental Crystal Structure Determination, 2000, DOI: 10.5517/cc51gqc.

[50] European Centre for Disease Prevention and Control, Antimicrobial resistance surveillance in Europe 2011. Annual Report of the European Antimicrobial Resistance Surveillance Network (EARS-Net). Stockholm, ECDC; (2012).

[51] M. A. Kohanski, D. J. Dwyer, J. J. Collins, Nat. Rev. Microbiol. 8 (2010) 423 – 435.

[52] R. E. W. Hancock, A. Nijnik, D. J. Philpott, Nat. Rev. Microbiol. 10 (2012) 243 – 254.

[53] K. M. O'Connell, J. T. Hodgkinson, H. F. Sore, M. Welch, G. P. Salmond, D. R. Spring, Angew. Chem. Int. Ed. 52 (2013) 10706-33.